VECTOR ANALYZERS FOR TECHNICAL AND MEDICAL DIAGNOSTICS

M. Min

Department of Electronics
Tallinn Technical University
Estonia, USSR

Abstract

Due to an extensive use of vector measurements in the diagnostics of various objects in the technical, biological, chemical and other fields, a need for a high-performance and flexible instrument — a vector analyzer — has arisen. In the present paper the architecture of vector analyzers based on discrete phase-sensitive demodulation of analog signals in the frequency range of 1 Hz to 1 MHz is considered.

The description of some typical experiments from the domain of electronic circuit fault analysis and medical diagnosis is given.

Keywords: vector analyzer, phase-sensitive demodulation.

Introduction

Vector measurements of complex impedances and admittances as well as complex gain factors of a variety of objects appear to be an effective method to diagnose their state, composition and nature (MEADE, 1983; KNELLER and BOROVSKIKH, 1986; PENNEY, 1986; SEN and SAEKS, 1979; MOSCHYTZ and HORN, 1981). To perform vector measurements, special measuring instruments: vector analyzers, known also as two-phase lock-in amplifiers (MEADE, 1983) are needed, which operate on the basis of phase-sensitive demodulation of the alternating signals to be measured (MEADE, 1983; MIN et al, 1986; MIN and PARVE, 1987).

In *Fig. 1.* a generalized structure of a vector analyzer is given consisting of a two-phase synchronous demodulator, connected to a vector computer and the object to be analyzed. The synchronous demodulator generates the alternating excitation signal S_{exc}, which is applied to the object. A shaded part to be studied is separated in the object where both the differential input signal S_{in} and the reference signal S_{ref} are obtained. Phase-sensitive demodulation is performed relatively to S_{ref}.
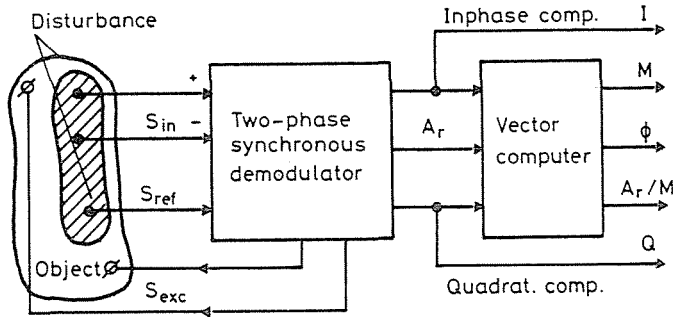
Fig. 1.   Block diagram of the vector analyzer and a typical measuring circuit

In the demodulation process the input signal is decomposed into inphase and quadrature components:

$$S_{\mathrm{in}}(t) = M \sin(\omega t + \phi) =$$
$$= (M \cos \phi) \sin \omega t + (M \sin \phi) \cos \omega t, \tag{1}$$

where amplitudes of inphase and quadrature components (I and Q) are obtained in the form of direct current components:

$$I = M \cos \phi, \tag{2}$$
$$Q = M \sin \phi, \tag{3}$$

which at a given frequency of $\omega = \omega_1$ appear as vector coordinates of the input signal S_{in} on the complex plane in *Fig. 2.*:

$$\dot{S}_{\mathrm{in}} = M e^{j\phi} = I + jQ, \tag{4}$$

where the magnitude is

$$M = \sqrt{I^2 + Q^2}, \tag{5}$$

and the phase is

$$\phi = \operatorname{arctg} \frac{I}{Q}. \tag{6}$$

We see that the arrangement of the coordinate system in *Fig. 2.* is determined not by vector S_{exc} of the excitation signal, but by vector S_{ref} of the reference signal.

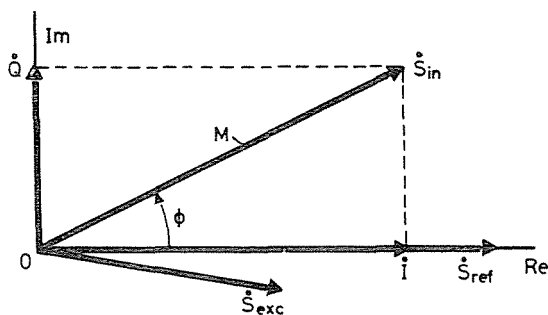$$S_{\mathrm{ref}}(t) = A_r \sin \omega_1 t. \tag{7}$$

Fig. 2. Vector diagram of the signals

The scale factor and orthogonality of the coordinate system are determined by the mutually quadrature and normalized coordinate signals

$$S_{c1}(t) = A_1 \sin(h\omega_1)t, \tag{8}$$

$$S_{c2}(t) = A_1 \cos(h\omega_1)t, \tag{9}$$

where $h = 1, 2, 3$ etc. is the series number of the analyzed harmonic component of the input signal, and A_1 is the amplitude unity. Signals (8) and (9) are formed strictly synchronously to the reference signal (7). Having multiplied the input signal (1) and the coordinate signal (8) and (9), and having smoothed the results obtained, we get inphase and quadrature components (2) and (3) of the hth harmonic component of the input signal:

$$I_h = \frac{1}{T} \int_0^T S_{\text{in}}(t) \cdot S_{c1}(t)dt, \tag{10}$$

$$Q_h = \frac{1}{T} \int_0^T S_{\text{in}}(t) \cdot S_{c2}(t)dt. \tag{11}$$

With the help of the vector computer, magnitude M_h and the phase of the hth harmonic component are calculated, see expressions (5) and (6), and amplitude gain factor A_r/M_h of the object and other necessary parameters are determined.

Due to the noise and external disturbances (*Fig. 1.*) superimposed on the input signal as well as on the reference signal, it is necessary to assure noise immunity of the analyzer with respect to both of the signals. This is achieved by a rational construction of a synchronous demodulator.

Two-Phase Synchronous Demodulator

The block diagram of the synchronous demodulator considered (MIN et al, 1983, 84, 87; PUNGAS et al, 1981), is given in *Fig. 3*. Characteristic elements of the diagram are the multiplying functional digital-to-analog converters (FDAC), two of which ($m = 3$) have three discrete states and act as the inphase ($0°$) and the quadrature ($90°$) synchronous detectors SD1 and SD2, while the third one ($m = 4$) operates as a source of the sine wave ($0°$) excitation signal S_{exc} with the amplitude E, where m is the number of discrete states of the FDAC.
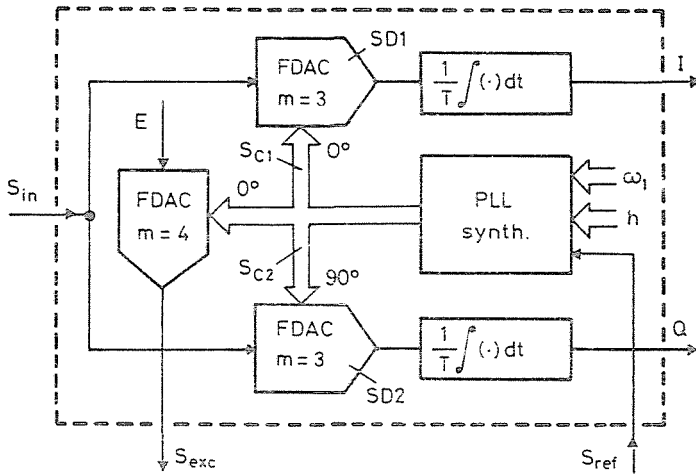

Fig. 3. Circuit diagram of the two-phase synchronous demodulator

As coordinate signals (8) and (9), corresponding code signals are used (*Fig. 4.*):

$$S_{c1} = \{S_I; S_{1,3}; S_{2,3}\}, \tag{12}$$

$$S_{c2} = \{S_Q; \overline{S_{2,3}}; \overline{S_{1,3}}\}. \tag{13}$$

The following code signal ($0°$) controls the third FDAC ($m = 4$):

$$S'_{c1} = \{S_I; S_{1,4}; S_{2,4}; S_{3,4}\}. \tag{14}$$

All code signals are synthesized with the help of the phase-locked loop (PLL) (MIN et al, 1986; MIN, 1985, 87). The frequency of code signals is
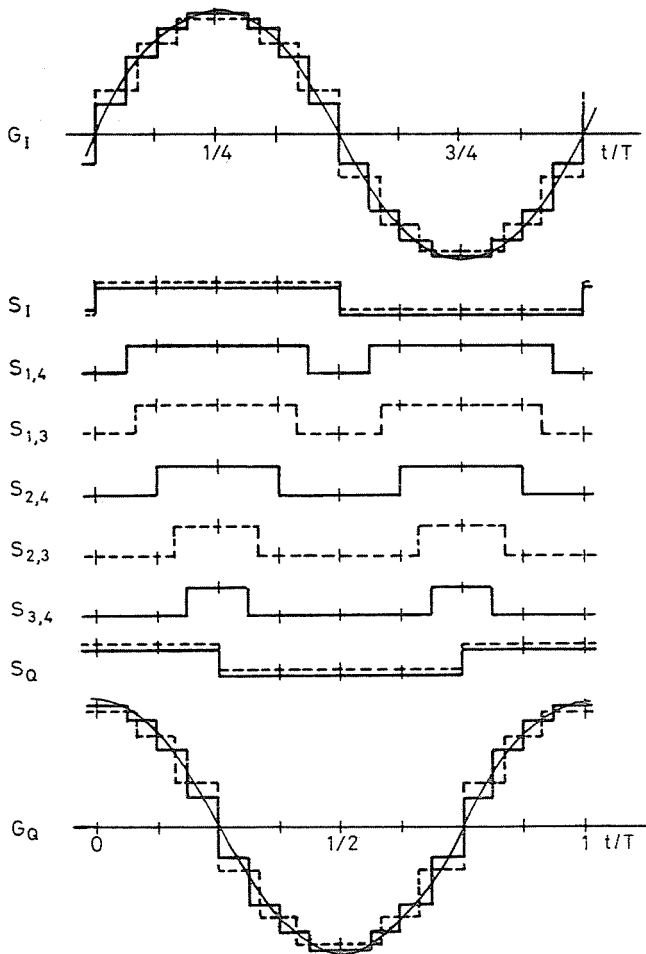
Fig. 4. Time diagrams of the variables G_I and G_Q and code signals for the number of approximation levels $m = 3$ (dashed lines) and $m = 4$ (continuous lines)

tuned to f_1 with the help of an external code, whereas the synchronization of phase and frequency in the PLL is performed by the reference signal S_{ref} (MIN et al, 1986). So, by setting the value for h, a possibility arises for vector analysis of the hth harmonic component of the input signal.

The FDAC, which operates as a synchronous detector $(m = 3)$, contains only three weighting resistors (*Fig. 5.*) with corresponding conductivities of $g_{1,3}$, $g_{2,3}$ and $g_{3,3}$. The resistors are switched on and off with the

help of current switches SW1, SW2 and SW3 operating under the control of code signals (12) or (13) from the output of the PLL to obtain corresponding sine- and cosine-like signals for conductivities $G_3 = G_I$ and $G_3 = G_Q$, see the dashed diagram lines in *Fig. 4*. Circuit design aspects are more closely described in the patent specification (MIN et al, 1983).

Hence, input voltage V_{in} is converted into weight current $i = V_{\mathrm{in}}G_3$, which, in turn, with the help of operational amplifiers with RC feedback and a summing converter of voltage V_0 to current i_0, yields the output signal.
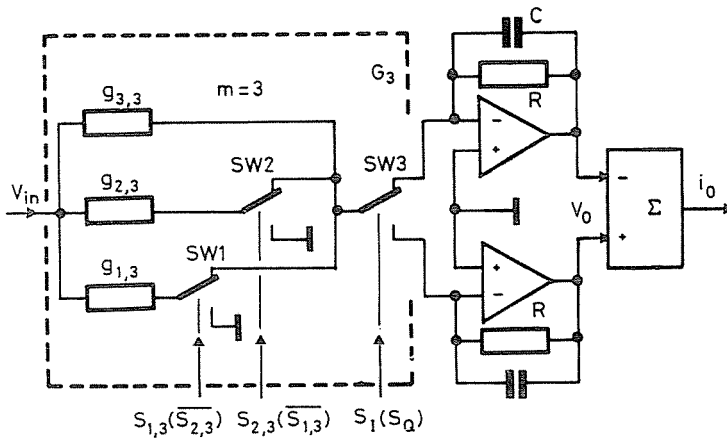
Fig. 5.   Circuit diagram of the functional DAC with three discrete levels $(m = 3)$

The FDAC with its four discrete levels $(m = 4)$ performs as the source of sine and cosine signals. It contains (*Fig. 6.*) four weighting resistors, switched by the current switches SW1, SW2, SW3, and the switch SW4 for the voltage $\pm E$. The switches are controlled by the code coordinate signal S'_{c1} (14). To obtain cosine signal, another coordinate signal has to be used:

$$S'_{c2} = \{S_Q; \overline{S_{3,4}}; \overline{S_{2,4}}; \overline{S_{1,4}}\}. \tag{15}$$

The value of conductivity G_4 of FDAC the changes corresponding to sine rule $G_4 = G_I$ or to cosine rule $G_4 = G_Q$, see continuous lines in *Fig. 4*. The weighted current $i_0 = EG_4$ is further converted into voltage V_{exc} with the help of current-to-voltage converter CV. Circuit description is given in the patent specifications (PUNGAS et al, 1981; MIN et al, 1984).

Vector analyzers of the family QUADRA, in which the above mentioned FDAC has found application, make it possible to carry out vector analysis of alternating current voltages and their higher harmonics
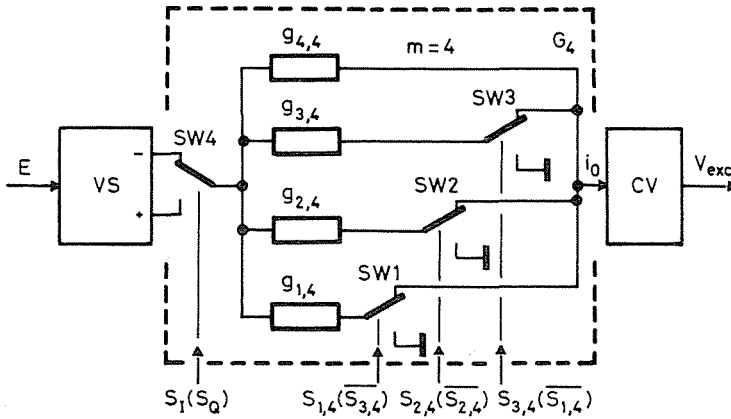
Fig. 6.   Circuit diagram of the functional DAC with four discrete levels ($m=4$)

($h = 1 \ldots 10$) in the range of 100 nV to 100 mV at frequencies from 1 Hz to 1 MHz. The dynamic range at the output is no less than 100 dB at the frequency of 1 kHz, and additive noise can exceed the full scale of the instrument up to 100,000 times. The noise-to-signal ratio for the reference input may be up to 0 dB.

Operation of FDACs

The functional digital-to-analog converters (FDAC) used in our design, with the number of discrete levels contained being only 3 or 4, are of extremely simple structure. However, these levels correspond to the determined values of the harmonic function (*Fig. 4.*) with a high accuracy (the error is less than ±0.05%), whereas the approximations are carried out so (MIN and PARVE, 1987), that the lower order harmonics should be absent in the spectra of functions G_3 and G_4.

To determine the values of separate discrete levels, the following formula is valid (MIN AND PARVE, 1987):

$$g_q = G_0 \sin \left[\frac{\pi}{4m} \cdot (2q - 1) \right], \tag{16}$$

where m is the number of approximating levels, and q is the ordinal number of the approximating level ($q = 1, 2, 3, \ldots, m$), while the minimal value of q corresponds to the lowest level of approximation.

4*

The spectral composition of approximated harmonic functions can be found according to a simple formula (MIN and PARVE, 1987):

$$k = 4mn \pm 1, \tag{17}$$

where n is integer ($n = 1, 2, 3, \ldots$), and the amplitudes A_k of the harmonics are:

$$A_k = \frac{A_1}{k}, \tag{18}$$

where A_1 is the amplitude of the first harmonic ($k = 1$).

Spectra of the functions G_I and G_Q at $m_1 = 3$ (continuous line) and at $m_2 = 4$ (dashed line) are shown in *Fig. 7.* Characteristically, the spectral lines in *Fig. 7.* do not coincide. Hence, a question arises if there are any coinciding spectral lines at different values of the number of approximation levels m_1 and m_2, and if so, what are their ordinal numbers k?
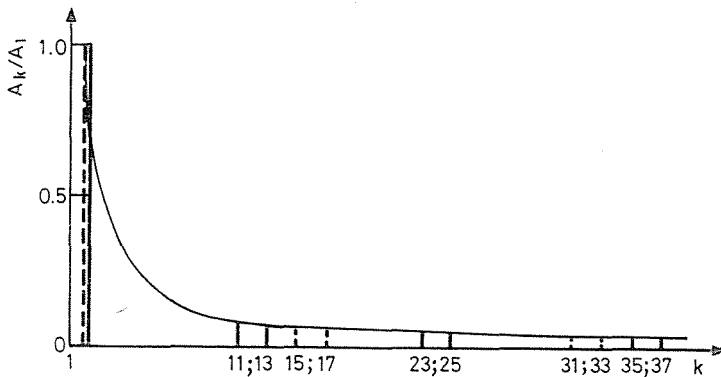
Fig. 7.   Amplitude spectra of harmonic function G_3 and G_4 approximated by three levels ($m = 3$, continuous lines) and four levels ($m = 4$, dashed lines)

On the basis of the formula (17), the following equation is obtained:

$$m_1 n_1 = m_2 n_2, \tag{19}$$

which is satisfied, if

$$n_1 = m_2 i \quad \text{and} \quad n_2 = m_1 i, \tag{20}$$

where $i = 1, 2, 3, \ldots$

Consequently, coinciding higher harmonics do exist, and on the basis of expressions (17) and (20) they have as ordinal numbers:

$$k = 4m_1 m_2 \pm 1. \tag{21}$$

Here $m_1 = 3$ and $m_2 = 4$, and hence, the coinciding harmonics of the functions G_3 and G_4 are:

$$k = 47, 49, 95, 97, 143, 145, \text{ etc.,} \tag{22}$$

with the amplitudes corresponding to formula (18).

The fact that only high frequency harmonics will coincide, could not be overemphasized for an efficient operation of the above-mentioned vector analyzer. As is well known, the synchronous demodulator is sensitive to only the harmonics of the input signal, which are contained in function G_3 (MEADE, 1983; MIN and PARVE, 1987). That is also the reason why it is sensitive only to the harmonics of the excitation signal, which coincide with harmonics of function G_4, see expressions (21) and (22). So,

$$Q_k = \frac{1}{k^2} \tag{23}$$

will serve as a relative sensitivity to these harmonics with the ordinal number k, as the multiplication of functions G_3 and G_4 is carried out within the process of synchronous demodulation. From expression (22) it can be seen that for any common harmonic, $Q_k < 0.05\%$. And, only as a consequence will a rough approximation of functions G_I and G_Q appear efficient (*Fig. 4.*).

High accuracy of the operation (error less than 0.1%) is guaranteed by a low number (3 and 4) of precision resistors (tolerance of $\pm 0.02\%$) used, whereas a good high frequency performance is guaranteed by using current switches and a low number of switching operations during one waveform period of functions G_I and G_Q (*Fig. 4.*). The dynamic range of the FDAC for analog input is 100 μV to 10 V at the frequency of 1 kHz.

Architecture and Operation of PLL Synthesizer

The phase-locked loop (PLL) is used for the synthesis of code coordinate signals S_{c1}, S'_{c1}, S_{c2} and S'_{c2}, see expressions (10–12) and (14), locked to the reference signal with a phase error $\phi_\epsilon < 0.1°$. Code signals are effective in the frequency range of 1 Hz to 1 MHz (MIN et al, 1986, 87), whereas

the noise level permitted, may reach the level of the useful reference signal S_{ref}.

The structure of PLL (*Fig. 8.*) encloses phase detector PD, which operates on the basis of the FDAC (see *Fig. 5.*), the lowpass filter LPF1, the voltage controlled oscillator VCO, the frequency divider FD having a dividing factor h and a code former of coordinate signals (*Fig. 4.*) with a frequency division ratio of 48, controlling all FDACs in the vector analyzer (*Fig. 3.*). For measuring the level of the reference signal S_{ref}, a synchronous detector SD on the basis of another FDAC is used. From the output of the SD through LPF2, a direct current signal is obtained which corresponds to amplitude A_r of the reference signal (7). This signal has also been used for automatic gain control, AGC.
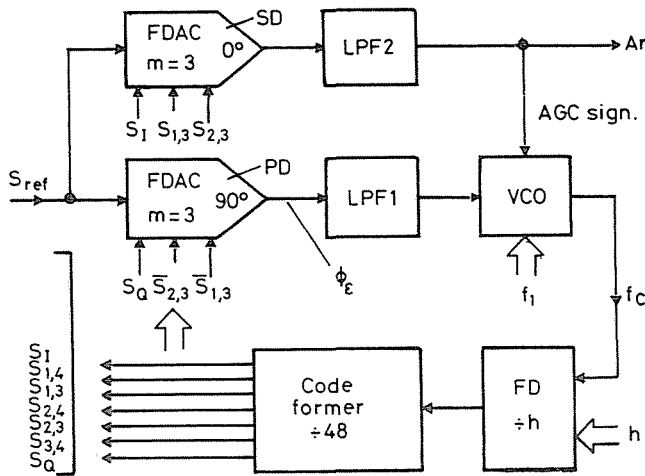
Fig. 8. Circuit diagram of the PLL synthesizer

LPF2 being a simple RC-filter, the LPF1 appears to be a more complex one with transfer function (MIN, 1985, 87):

$$F(s) = \frac{\tau_2 s + 1}{T_F s (\tau_3 s + 1)}. \tag{24}$$

As the gain of PD has a sine form, the output signal of PD is expressed as:

$$S_{\text{PD}} = G_{\text{PD}} \cdot A_r \sin \phi_\epsilon, \tag{25}$$

where $\quad G_{\text{PD}}$ — gain of the PD,

$\qquad A_r$ — amplitude of the reference signal, and

$\qquad \phi_\epsilon$ — phase-lock error of coordinate signals.

As signal (25) is dependent on A_r, automated gain control (AGC) of the PLL is needed.

If the phase error ϕ_ϵ is small, the PLL may be linearized, $\sin \phi_\epsilon \approx \phi_\epsilon$, and characterized by the open-loop transfer function (MIN, 1985):

$$G(s) = F(s) \cdot L(s) = \frac{\tau_2 s}{T_A^2 s^2 (\tau_3 s + 1)}, \tag{26}$$

where

$$L(s) = \frac{1}{T_L s} \tag{27}$$

appears as the open-loop transfer function of PLL without LPF1, and time constant

$$T_A = \sqrt{T_F \cdot T_L}. \tag{28}$$

The transfer function (26) may be expressed with the help of relative parameters

$$\nu = \frac{\tau_2}{\tau_3}, \quad \chi = \frac{\tau_2}{T_A}, \tag{29}$$

their optimization, in respect to the best response speed and noise immunity of PLL (MIN, 1985, 87), gives the following results:

$$\text{opt}[\nu] = 5 \ldots 7, \tag{30}$$

$$\text{opt}[\chi] = \frac{\text{opt}[\nu]}{3} \sqrt{\frac{2}{\text{opt}[\nu] - 3}}. \tag{31}$$

The frequency of the PLL synthesizer is set with the help of codes f_1, the frequency of the main harmonic of the input signal, and h, the ordinal number of the analyzed harmonic. The exact frequency and phase lock of the VCO is carried out automatically in the PLL and the phase error ϕ_ϵ being led to minimum.

The clock frequency from the VCO output

$$f_c = 48 h f_1 \tag{32}$$

reaches 48 MHz at the maximum signal frequency $f_1 = 1\text{MHz}$, if $h = 1$.

Diagnostics and Regulation of Electronic Circuits

Problems concerning the diagnostics of elements and units in analog elec-
tronic circuits have been examined in a number of papers (SEN and SAEKS,
1979; MOSCHYTZ and HORN, 1981). Compared with other experimental
methods the vector measurements have obvious advantages in the diag-
nostics and regulation of frequency dependent circuits, e.g. high order
active filters. As can be seen from (MOSCHYTZ and HORN, 1981, Ch.6),
the parameter deviation of circuit elements (resistors, capacitors etc.) is
much better reflected in phase and in quadrature components than in the
magnitude. This is especially true for circuits of non-minimal-phase type.

A typical circuit under test, where any part (see A2) of the device
may be taken as an object of diagnostics, is given in *Fig. 9*. This is pos-
sible through a high sensitivity of the vector analyzer to the measuring
signal, and by its non-sensitivity to nonlinear distortions and external dis-
turbances.

High sensitivity and noise immunity enable e.g. to carry out the anal-
ysis of a complex transfer function $G(j\omega)$, i.e. the Nyquist diagram of an
open-loop high-gain amplifier without switching off the feedback (*Fig. 10.*).
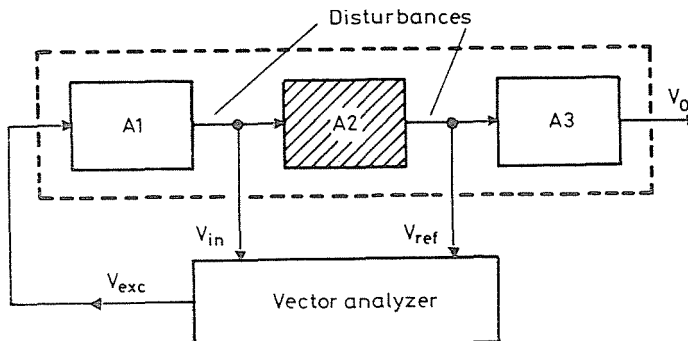
Fig. 9. Application of the vector analyzer for diagnostics of electric circuits

A more detailed description of the diagnostics and regulation of a
twin-T bridge is given here (*Fig. 11.*). In the ideal case resistors and ca-
pacitors have the following relative values: $R_1 = R_2 = R$ and $R_3 = 0.5R$;
$C_1 = C_2 = C$ and $C_3 = 2C$; load resistance $R_L = 1000R$. A bridge like that
has a zero gain at the frequency $\omega = 1/RC$.

In reality, deviation from the nominal values of the parameters are
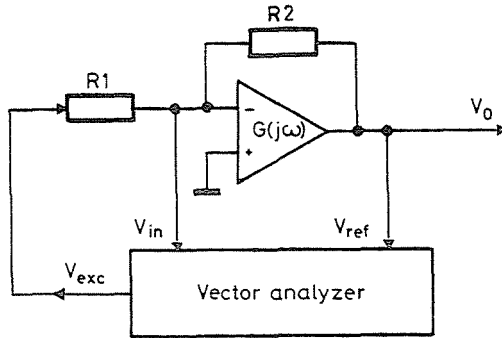present. Analysis and experience show that the bridge capacitor C_3 and

Fig. 10. Measuring of the open-loop complex transfer function of a high gain amplifier
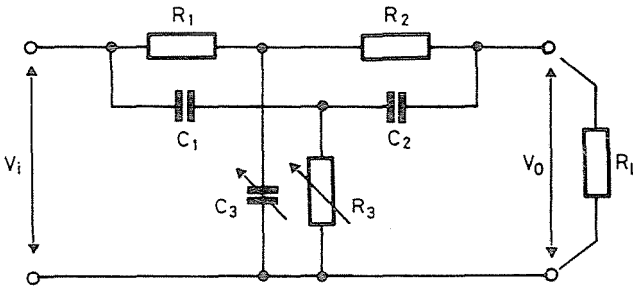

Fig. 11. Circuit diagram of the twin-T bridge

resistor R_3 should be regulated for balancing. It may be convenient to do it on the basis of inphase and quadrature components of output voltage V_0.

In *Fig. 12.* gain and phase frequency responses of a twin-T bridge are given with deviation $\delta R_3 = \pm 5\%$ of resistor R_3. At $RC = 1$ s the bridge sensitivity may be expressed as follows:

$$W_{R_3} = \frac{\pm \delta R_3}{-(4 \pm \delta R_3) + j(1 \pm \delta R_3)},\tag{33}$$

and phase ϕ at small deviations δR_3 has the following values:

$$\phi = \operatorname{arctg}(\pm 0) - \operatorname{arctg}(-1),\tag{34}$$
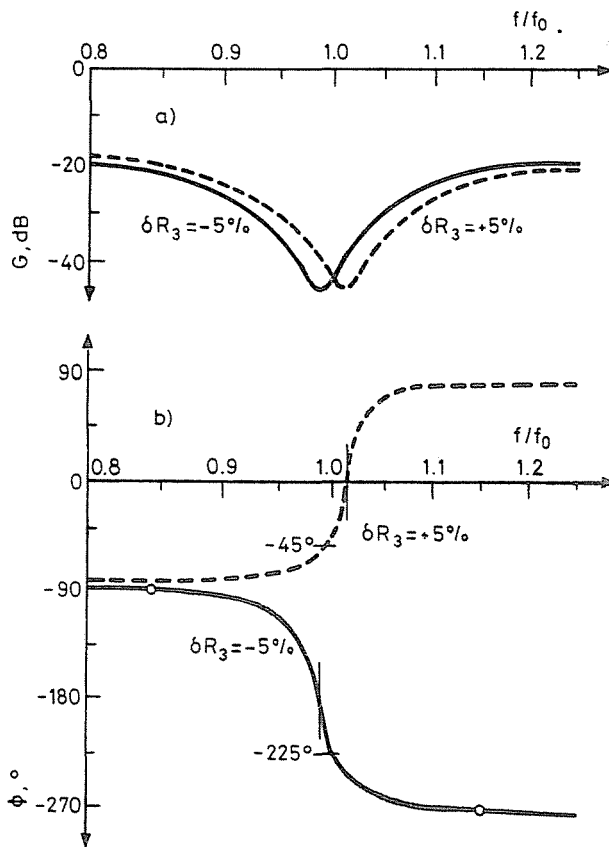
i.e. at relative frequency $f/f_0 = 1$

$$\phi = \begin{cases} -45° & \text{for } \delta R_3 > 0, \\ -225° & \text{for } \delta R_3 < 0, \end{cases}\tag{35}$$

independently from the value of deviation (*Fig. 12.*).

For corresponding deviations δC_3 of capacitor C_3 , the phase values are the following:

$$\phi = \begin{cases} 225° \text{ for } \delta C_3 > 0, \\ 45° \text{ for } \delta C_3 < 0. \end{cases} \tag{36}$$

At the nominal frequency the phase shift will be $0°$ or $-180°$, correspondingly (*Fig. 12.*).

Fig. 12. Gain (A) and phase (B) frequency responses of the twin-T bridge at the deviations of the resistor $\delta R_3 = \pm 5\%$

On the basis of this example it should not be difficult to see the advantages of vector measurements in the diagnostics of frequency-dependent electronic circuits.

To the typical problems to be solved belongs also the analysis of non-linearities of high-performance amplifiers, which have a coefficient of non-linear distortions less than 0.1%. In that case it would be necessary to apply the compensation method of measurement (*Fig. 13*).

As can be seen in *Fig. 7.*, in an ideal case the spectrum of excitation signal S_{exc} does not contain higher harmonics with ordinal numbers up to 15 at $m = 4$. However, actually, due to technical imperfections, the level of these possible harmonics may be as high as 0.01 to 0.1% of the excitation signal due to an inaccuracy of the weighting resistors in the FDAC (*Fig. 6.*). As a result, a situation arises where the excitation signal itself contains more harmonics than caused by the object. The solution is an automatic compensation of the main component as well as higher harmonics of the excitation signal S_{exc}. The realization is performed by a controllable gain around the value of G_A^{-1} of voltage divider VD, where G_A is the gain of the tested amplifier (see *Fig. 13.*). Accurate compensation is realized by feedback through the digital integrator DI, the output signal of which may be fixed.
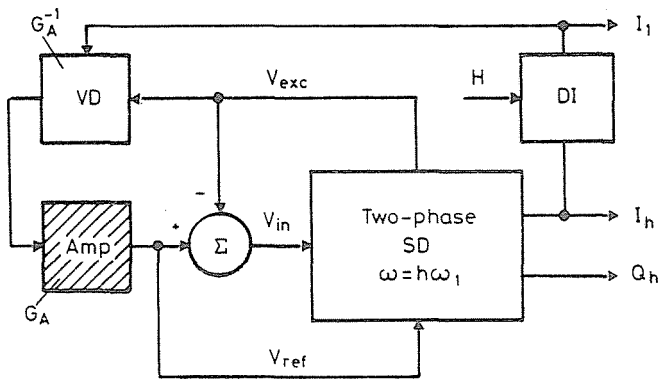
*Fig. 13.* Measuring nonlinear distortions of an electronic amplifier

If some phase shift is produced by the object, additional compensation through the phase shifter is necessary. As a result, 50 to 100-fold compensation enables to detect nonlinear distortions of the order of 0.001% by separately measuring several higher harmonics at frequencies $h\omega_1$.

Applying the above-mentioned method of compensation, we can also measure nonlinearities of separate units of more complex circuits, as, for

example, those of the circuit in *Fig. 9*. In that case nonlinear distortions of
the preceding units will be compensated, in our case of unit $A1$ in *Fig. 9*.

Vector Measurements in Medical Diagnostics

The application of vector measurements in medical diagnostics is mainly
based upon the measurement and analysis of bioelectrical impedances
(KNELLER and BOROVSKIKH, 1986; PENNEY, 1986). Among the most com-
mon experiments are, for example, the determination of liquid content in
organs and tissues of the body, study of the speed and capacity of the blood
circulation (hemodynamics) in different organs of the human body. Hemo-
dynamics is performed by measuring the changes of reactive and active
components of bioimpedance in the pulse rhythm (reoplethismography).
For example, the active resistance of the blood-vessel impedance is inversely
proportional to the speed of blood circulation in a vessel, whereas changes
in electrical capacitance in the pulse rhythm show the vessel elasticity.
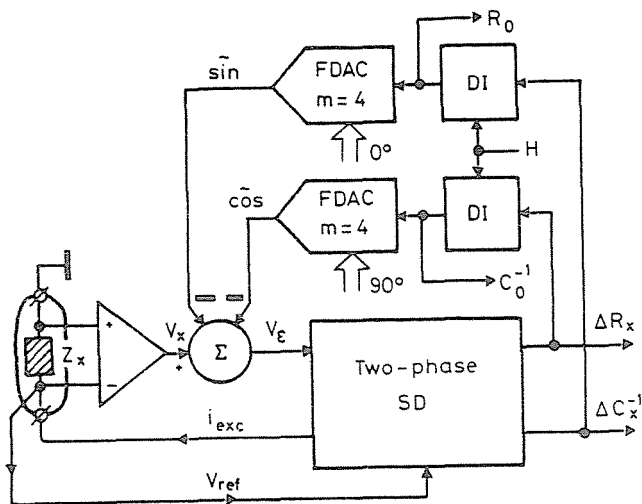
Fig. 14. Measuring the bioelectrical impedance

In *Fig. 14.* the compensation circuit is shown for measuring base compo-
nents R_0 and $(\omega C_0)^{-1}$ of the bioelectrical impedance Z_x and its relatively
rapid pulse deviations ΔR_x and ΔC_x. Due to inertia of digital integra-
tors DI, the compensation is performed for constant or slowly changing

base components R_0 and C_0. Direct measurements are realized for relatively rapid pulse deviations ΔR_x and ΔC_x over the range 0.01 to 1.0%. The circuit in *Fig. 14.* appears to be efficient when analysing deviations of impedance components not only in the field of medicine, but also when performing other experiments, e.g. in corrosion measurements (GABRIELLI, 1987) in the field of electrochemistry.

Conclusion

A wide variety of applications for the above-described vector analyzers enables to use them in technical and medical diagnostics and in scientific experiments in the fields of physics, electrochemistry, material study etc.

Wide input dynamic range (100 dB) and superior noise immunity — noises may exceed the instrument range up to 100 000 times — have been achieved thanks to discrete processing of the analog signals on the basis of multiplying functional digital-to-analog converters.

References

GABRIELLI, C. (1987): Mesure de corrosion, c'est aussi une affaire d'impedance (Measure of corrosion is also a matter of impedance). *Mesures*, No. 12, 5 octobre 1987. pp. 80–93. (In French)

KNELLER, V. YU. – BOROVSKIKH. L. P. (1986): Determination of Parameters of the Multielement Two-Pole Circuits. Moscow, Energoatomizdat. (in Russian)

MEADE, M. L. (1983): Lock-in Amplifiers: Principles and Applications. London, Peter Peregrinus.

MIN, M. (1985): A Method for Design of the Time Optimal Third Order Phase Locked Loop. *Proc. 7th European Conf. on Circuit Theory and Design, ECCTD'85* (Prague), Sept. 2–5, Part 1, pp. 325–328.

MIN, M. (1987): Minimization of Transient Time in the Third Order Phase-Locked Loop. *Proc. 8th European Conference on Circuit Theory and Design, ECCTD'87* (Paris), Sept. 1–4, Part 2, pp. 835–840.

MIN, M. – PARVE, T. – PUNGAS, T. – HÄRM, H. (1983): Quadrature Stepwave Frequency Converter. US Patent No 4.409.555, Oct. 11, 1983.

MIN, M. – PARVE, T. – PUNGAS, T. (1984): Electrical Signal Converter with Step Variable Gain. US Patent No. 4.473.802, Sept. 25, 1984.

MIN, M. – RONK, A. – SILLAMAA, H. (1986): Adaptive Control of Frequency and Phase in a Vector Analyzer. *Proc. 5th IMEKO TC7 Symposium on Intelligent Measurement*, Jena, GDR, June 10-14, 1986. pp. 251–256.

MIN, M. – PARVE, T. (1987): Phase-Locked Signal Processing in Vector Analyzer. *Proc. 6th IMEKO TC7 Symposium on Signal Processing in Measurement*, Budapest, Hungary, June 10-12, 1987. Nova Science Publishers, Commack, NY. pp. 97–101.

MOSCHYTZ, G. S. – HORN, P. (1981): *Active Filter Design Handbook*. New York, John Wiley and Sons.

PENNEY, B. C. (1986): Theory and Applications of Electrical Impedance Measurements. *CRC Critical Reviews in Biomedical Engineering* (USA), Vol. 13, No 3, pp. 227–281.
PUNGAS, T. – PARVE, T. – MIN, M. (1981): Reference Voltage Source. US Patent No. 4.281.281, July 28, 1981.
SEN, N. – SAEKS, R. (1979): Fault Diagnosis for Linear Systems via Multifrequency Measurement. *IEEE Trans. on Circuits and Systems,* Vol. CAS-26, No 7, July 1979, pp. 457–485.

Address:

Dr. Mart MIN
Department of Electronics
Tallinn Technical University
Ehitajate tee 1, Tallinn, SU-200108
Estonia, USSR